Journal of Marine Science and Technology

Volume 21 | Issue 6 Article 1

AN EFFECTIVE COLOR-DIFFERENCE-BASED DEMOSAICKING METHOD

Yea-Shuan Huang
Department of Computer Science and Information Engineering, Chung-Hua University, Hsinchu, Taiwan, R.O.C, huang@chu.edu.tw

Sheng-Yi Cheng
Department of Computer Science and Information Engineering, Chung-Hua University, Hsinchu, Taiwan, R.O.C

Recommended Citation
Huang, Yea-Shuan and Cheng, Sheng-Yi (2013) "AN EFFECTIVE COLOR-DIFFERENCE-BASED DEMOSAICKING METHOD," *Journal of Marine Science and Technology*: Vol. 21: Iss. 6, Article 1.
DOI: 10.6119/JMST-012-0829-1
Available at: https://jmstt.ntou.edu.tw/journal/vol21/iss6/1

AN EFFECTIVE COLOR-DIFFERENCE-BASED DEMOSAICKING METHOD

Acknowledgements

The author acknowledges the financial support of the Na- (a) Original (b) BI (c) ACPI (d) ECI (e) proposed ECDB Fig. 8. Enlarged parts of the demosaicked image corresponding to the Parrots: (a)The original image, (b) BI, (c) ACPI, (d) ECI, and (e) the proposed ECDB. tional Science Council (NSC 100-2221-E-216-031 and NSC 100-2622-E-216-001-CC3), ROC.

Journal of Marine Science and Technology, Vol. 21, No. 6, pp. 623-630 (2013)
DOI: 10.6119/JMST-012-0829-1

AN EFFECTIVE COLOR-DIFFERENCE-BASED DEMOSAICKING METHOD

Yea-Shuan Huang and Sheng-Yi Cheng

Key words: color filter array, demosaicking, interpolation.

ABSTRACT

This paper proposes an effective color-difference-based (ECDB) interpolation algorithm for color filter array (CFA) image demosaicking. A CFA image consists of a set of spectrally selective filters which are arranged in an interleaved pattern such that only one color component is sampled at each pixel location. To improve the quality of reconstructed full-color images from CFA images, the ECDB algorithm first analyzes the samples immediately around a missing green pixel to determine suitable samples for interpolating the value of this missing green pixel. After finishing the interpolation operations of all the missing green pixels, a complete green plane (i.e $\bar{G}$ plane) is obtained. The ECDB algorithm then makes use of the high correlation between the *R*, *G*, and *B* planes to produce the red–green and blue–green color difference planes and further reconstructs the red and blue planes in successive operations. Because the green plane provides twice the information of the red and blue planes, the algorithm uses the information of the green plane more than that of the red/blue planes so that the full color image can be reconstructed more accurately. In essence, the ECDB algorithm uses the red–green and blue–green color difference planes, and develops different conditional operations according to the horizontal, vertical, and diagonal neighboring pixel information with a suitable weighting technique. The experimental results demonstrate that the proposed algorithm performed extremely well.

I. INTRODUCTION

Nowadays, most of electronic devices such as digital still cameras, mobile phones, and PDAs use a single image sensor to capture digital images, which usually consist of three color components (red, green, and blue) at each pixel location. However, the surface of the single image sensor is covered with a color filter array (CFA) [6]. A CFA image consists of a set of spectrally selective filters [5, 10] which are arranged in an interleaved pattern such that only one color component is sampled at each pixel location. In order to render a full color image, an image interpolation algorithm is performed to estimate the other two missing color components and the image interpolation is called a CFA demosaicking algorithm (spectral interpolation).

To obtain a good demosaicked color image, a lot of demosaicking algorithms have been proposed, such as Bilinear Interpolation (BI) [3], Cubic Spline Interpolation (CSI) [9], Nearest-Neighbor Replication (NNR) [2], Edge-Adaptive Demosaicking Algorithm (EADA) [11], Correlation-Correction Approach (CCA) [7], Demosaicked Image Postprocessing Using Local Color Ratios [4], etc. Although, these single plane interpolation methods are easy to implement, they produce severe color artifacts around sharp areas. Recently, another method called Edge-Sensing Correlation-Correction (ESCC) has been proposed [8]. It firstly interpolates green missing pixels using eight neighboring green samples with a weighting technique, which considers the edges in all possible directions, i.e. diagonal, horizontal, and vertical. Next, it interpolates the missing red/ blue pixels by exploiting interplane color difference (red minus green/ blue minus green), which assumes that the hue does not abruptly change in a local area. The ESCCcan produce pleasing demosaicked images to human vision in most of cases. However, there are considerable false colors occurred at thin line areas of demosaicked image because the ESCC uses unsuitable samples to estimate the color values of missing pixels.

In this paper, we propose an effective demosaicking algorithm to reconstruct full-color images from CFA images based on a Bayer CFA pattern, and the reconstructed image has a very satisfactory visual quality. The proposed demosaicking algorithm is a new kind of effective color-difference-based interpolation (ECDB) demosaicking algorithm. The ECDB algorithm starts from the green plane to produce a reconstructed full-color image because the green plane provides twice the information of the red and blue planes. Therefore, when interpolating the green missing pixels, the ECDB algorithm makes use of neighboring samples to analyze the edge direction (vertical, horizontal or diagonal), then, according to

Paper submitted 05/01/11; revised 06/05/12; accepted 08/29/12. Author for correspondence: Yea-Shuan Huang (e-mail: huang@chu.edu.tw).
Department of Computer Science and Information Engineering, Chung-Hua University, Hsinchu, Taiwan, R.O.C.

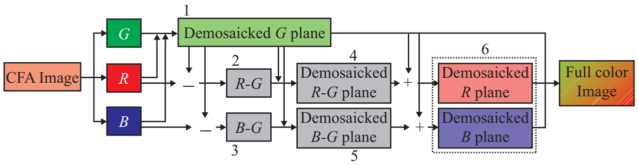

Fig. 1. Flowchart of the ECDB algorithm.

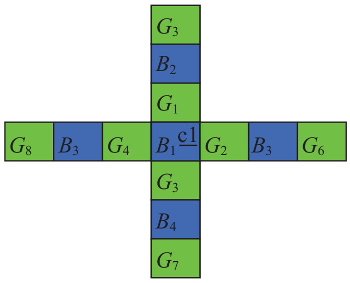

Fig. 2. Configuration of related pixels for estimating the green value of a pixel located at "c1".

specially designed operations, selects suitable samples for estimating the missing green pixel. Once the green plane is produced, the ECDB algorithm exploits both the demosaicked green plane and the original red/blue planes to produce red–green and blue–green color different planes. The the color different planes are then interpolated by using neighboring samples with a suitable weighting technique. Finally, by using the green plane, red–green and blue–green color difference planes high-quality demosaicked full-color images are reconstructed.

II. PROPOSED SCHEME

1. Demosaicking Procedure of the Green Plane

Fig. 1 shows the flowchart of the proposed ECDB algorithm. The ECDB algorithm starts with the procedures for recovering a CFA image using the demosaicked green plane. Then it exploits the *R-G* and *B-G* color difference planes to reconstruct the red and blue planes, respectively.

During the interpolation of the green plane, the pixels immediately around a currently processing pixel are considered. In general, high continuity neighboring pixels will have higher attribute (such as color or texture) consistency than low continuity neighboring pixels. To interpolate the missing color value of a pixel A only the pixels with high attribute consistency from all the neighboring pixels of A are chosen and the neighboring pixels with low attribute consistency are abandoned. Centered around pixel A, a region E of 7×7 pixels is defined. For each pixel A, the edge strength is used to measure the continuity and consistency among its neighboring pixels, and also use the edge strengths of different directions to determine the consistency direction (horizontal or vertical) of its corresponding region E. Obviously, the direction with the weaker edge strength probably corresponds to the consistency direction. If both vertical and horizontal edge strengths are very weak, then the region will be a smooth region. On the contrary, if both vertical and horizontal edge strengths are strong, then the region will be a complex region. Conceptually to interpolate the missing color value of pixel A, only the pixels along the consistency direction are used. However, even along the consistency direction probably only a part of pixels are truly consistent. Therefore, region E is divided into five different cases so that more appropriate pixels can be chosen. Case 1, the consistency direction is horizontal but only the right or left half of E is consistent. Case 2, the consistency direction is vertical but only the upper or lower half of E is consistent. Case 3, the consistency direction is horizontal and both the right and left half of E are consistent. Case 4, the consistency direction is vertical and both the upper and lower half of E are consistent. Case 5, both horizontal and vertical directions are either consistent or not. Based on the above judgment, the following mechanism is designed to interpolate the missing green. In the designed mechanism, a novel weighting technique was also designed to give each chosen pixel sample a suitable weight value for calculation.

Fig. 2 displays the configuration of related pixels for estimating the green value of the pixel located at "c1". Because the Bayer pattern has only one color value at each pixel location, two color values for each pixel are missing and they need to be estimated. In this section, interpolating the green color value on the blue plane is presented in detail, which is similar to interpolating the green color value on the red plane.

2. Principle of Variable Naming

In the proposed algorithm, a few variables are used. In order to understand these variables more easily, variable naming is introduced in this section. When defining a variable, it usually contains an abbreviated prefix, superscript and suffix. For the prefix, 'e' denotes "edge strength", 'w' denotes "weight", and 'd' denotes "demosaicked value". For the superscript, 'r', 'g', and 'b' denote the red, the green and the blue, respectively. Also, 'r-g' denotes the color difference of the red and the green, 'b-g' denotes the color difference of the blue and the green, 'gb' denotes the green channel referencing to the blue value, 'rb' denotes the color difference 'r-g' channel referencing to the blue value, 'rg' denotes the color difference 'r-g' channel referencing to the green value, and 'a' denotes "adaptive" to represent more than one color channel being used to interpolate a missing value. For the suffix, only the direction attribute, weight attribute, and the summation attribute appear. In the suffix, symbol 'w' denotes the weight attribute, symbol 's' denotes the summation attribute, and there are 12 direction-related attributes which are listed in Table 1 with their names and their corresponding symbols. For example, variable $e_{|}^{g}$ denotes the vertical edge strength computed from the green channel.

If the estimated value on the horizontal direction has high attribute consistence for both sides (left side and right side),

Table 1. List of suffix attributes and symbols.

Suffix Attribute	Symbol	Suffix Attribute	Symbol	Suffix Attribute	Symbol
Vertical	|	Top	↑	T-right	→↑
Horizontal	—	Bottom	↓	T-left	←↑
Diagonal	/	Left	←	B-right	→↓
R-diagonal	\	Right	→	B-left	←↓

an equal weight value is given to both side; otherwise, different weight values are given to both sides. The same concept can be applied on the vertical direction. Let $e^{gb}_{|}$, $e^{g}_{\uparrow}$ and $e^{g}_{\downarrow}$ be the blue vertical edge strength, green the color upper edge strength and also the lower edge strength of this configuration, respectively. Let e^{gb}_{-}, $e^{g}_{\rightarrow}$ and $e^{g}_{\leftarrow}$ be the blue horizontal edge strength, green the right edge strength and also the left edge strength of this configuration, respectively. The values of $e^{gb}_{|}$, $e^{g}_{\uparrow}$, $e^{g}_{\downarrow}$, e^{gb}_{-}, $e^{g}_{\rightarrow}$ and $e^{g}_{\leftarrow}$ are computed by Eq. (1) as

$$
\begin{aligned}
e^{gb}_{|} &= \left|2*B_1-B_2-B_4\right|,\\
e^{g}_{\uparrow} &= \left|G_1-G_3\right|+2*\left|G_1-G_5\right|,\\
e^{g}_{\downarrow} &= \left|G_1-G_3\right|+2*\left|G_3-G_7\right|,\\
e^{gb}_{-} &= \left|2*B_1-B_3-B_5\right|,\\
e^{g}_{\rightarrow} &= \left|G_2-G_4\right|+2*\left|G_2-G_6\right|,\\
e^{g}_{\leftarrow} &= \left|G_2-G_4\right|+2*\left|G_4-G_8\right|
\end{aligned}
\tag{1}
$$

Also, let $e^{g}_{|}$ and e^{g}_{-} be the edge strength values of the vertical and horizontal directions of this configuration, respectively. The value of $e^{g}_{|}$ is according to the calculation of $e^{gb}_{|}$, $e^{g}_{\uparrow}$ and $e^{g}_{\downarrow}$, and the value of e^{g}_{-} is according to the calculation of e^{gb}_{-}, $e^{g}_{\rightarrow}$ and $e^{g}_{\leftarrow}$. The above two edge strengths can be computed by Eq. (2) as

$$
e^{g}_{|} = 1+e^{gb}_{|}+\frac{e^{g}_{\uparrow}+e^{g}_{\downarrow}}{2},\quad e^{g}_{-} = 1+e^{gb}_{-}+\frac{e^{g}_{\rightarrow}+e^{g}_{\leftarrow}}{2}. \tag{2}
$$

Let d^{g}_{-}, $d^{b}_{\rightarrow}$ and $d^{b}_{\leftarrow}$ be three estimated horizontal-direction variables which are used to calculate the estimated missing green value $\hat{d}_{|-}$, $w^{g}_{\rightarrow}$ and $w^{g}_{\leftarrow}$ be the weight values of $d^{b}_{\rightarrow}$ and $d^{b}_{\leftarrow}$, $d^{g}_{|}$ be the estimated values of vertical direction, $d^{b}_{\uparrow}$ be the difference of B_1 and B_2, $d^{b}_{\downarrow}$ be the difference of B_1 and B_4, $w^{g}_{\uparrow}$ and $w^{g}_{\downarrow}$ be the weight values of $d^{b}_{\uparrow}$ and $d^{b}_{\downarrow}$. The 10 parameters (d^{g}_{-}, $d^{b}_{\rightarrow}$, $d^{b}_{\leftarrow}$, $w^{g}_{\leftarrow}$, $w^{g}_{\rightarrow}$, $d^{g}_{|}$, $d^{b}_{\uparrow}$, $d^{b}_{\downarrow}$, $w^{g}_{\uparrow}$ and $w^{g}_{\downarrow}$) are calculated as below:

$$
\begin{aligned}
&d^{g}_{-} = \frac{G_2+G_4}{2},\ d^{b}_{\rightarrow} = \frac{B_1-B_3}{4},\ d^{b}_{\leftarrow} = \frac{B_1-B_5}{4},\\
&d^{g}_{|} = \frac{G_1+G_3}{2},\ d^{b}_{\uparrow} = \frac{B_1-B_2}{4},\ d^{b}_{\downarrow} = \frac{B_1-B_4}{4}
\end{aligned}
\tag{3}
$$

$$
w^{g}_{\leftarrow} = \frac{e^{g}_{\rightarrow}}{e^{g}_{\rightarrow}+e^{g}_{\leftarrow}},\ w^{g}_{\rightarrow} = 1-w^{g}_{\leftarrow},\ w^{g}_{\uparrow} = \frac{e^{g}_{\downarrow}}{e^{g}_{\uparrow}+e^{g}_{\downarrow}},\ w^{g}_{\downarrow} = 1-w^{g}_{\uparrow} \tag{4}
$$

Let d^{a}_{w-} and $d^{a}_{w|}$ be the estimated values of horizontal and vertical directions with weight, respectively. d^{a}_{-} and $d^{a}_{|}$ are the estimated values of horizontal and vertical directions without weight, respectively. It can be calculated as bellow:

$$
\begin{aligned}
&d^{a}_{w-} = d^{g}_{-}+w^{g}_{\leftarrow}\times d^{b}_{\leftarrow}+w^{g}_{\rightarrow}\times d^{b}_{\rightarrow},\ d^{a}_{w|} = d^{g}_{|}+w^{g}_{\uparrow}\times d^{b}_{\uparrow}+w^{g}_{\downarrow}\times d^{b}_{\downarrow},\\
&d^{a}_{-} = d^{g}_{-}+d^{b}_{\rightarrow}+d^{b}_{\leftarrow},\ d^{a}_{|} = d^{g}_{|}+d^{b}_{\uparrow}+d^{b}_{\downarrow}.
\end{aligned}
\tag{5}
$$

Then, the central green missing sample "c1" can be estimated by the following Equation:

$$
\hat{d}^{g} = \begin{cases}
d^{a}_{w-}, & \text{if } e^{g}_{|}/e^{g}_{-} > R \text{ and } (e^{g}_{|}+e^{g}_{-}) > T_1 \text{ and } e^{g}_{-} < T_2 \text{ and } \left|e^{g}_{\rightarrow}-e^{g}_{\leftarrow}\right| > D_{eg};\\
d^{a}_{w|}, & \text{if } e^{g}_{-}/e^{g}_{|} > R \text{ and } (e^{g}_{|}+e^{g}_{-}) > T_1 \text{ and } e^{g}_{|} < T_2 \text{ and } \left|e^{g}_{\uparrow}-e^{g}_{\downarrow}\right| > D_{eg};\\
d^{a}_{-}, & \text{if } e^{g}_{|}/e^{g}_{-} > R \text{ and } (e^{g}_{|}+e^{g}_{-}) > T_1 \text{ and } e^{g}_{-} < T_2 \text{ and } \left|e^{g}_{\rightarrow}-e^{g}_{\leftarrow}\right| <= D_{eg};\\
d^{a}_{|}, & \text{if } e^{g}_{-}/e^{g}_{|} > R \text{ and } (e^{g}_{|}+e^{g}_{-}) > T_1 \text{ and } e^{g}_{|} < T_2 \text{ and } \left|e^{g}_{\uparrow}-e^{g}_{\downarrow}\right| <= D_{eg};\\
d^{a}_{|}\times w^{g}_{|}+d^{a}_{-}\times w^{g}_{-}, & \text{otherwise}.
\end{cases}
\tag{6}
$$

where $\hat{d}^{g}$ is the estimated value for the green missing pixel on the red or blue sample location at "c1". In Eq. (6), R, T_1, T_2 and D_{eg} are four threshold values. R is the threshold for the ratio of $e^{g}_{|}$ and e^{g}_{-}. If the value of $e^{g}_{|}/e^{g}_{-}$ is larger than $\boldsymbol{R}$, it means the configuration of "c1" has relatively high continuity in the horizontal direction, else if the value of $e^{g}_{-}/e^{g}_{|}$ is larger than R, then it means the configuration of "c1" has relatively high continuity on the vertical direction, otherwise, there is no obvious horizontal and vertical continuity at position "c1". If the edge strength $|e^{g}_{|}+e^{g}_{-}|$ is larger than T_1, it means the central pixel at "c1" position is located at a non-smooth area with low continuity in either horizontal or vertical direction; otherwise pixel "c1" is located at a smooth area with high continuity in both horizontal and vertical directions. If the edge strength (either e_{-}^{g} or $e_{|}^{g}$) is less than T_2, it means pixel "c1" is located at a non-complex area with high continuity in either horizontal or vertical direction; otherwise, "c1" is located at a complex area with low continuity in both horizontal and vertical direction. $e_{\rightarrow}^{g}$ and $e_{\leftarrow}^{g}$ are the edge strengths of the horizontal direction for the right side and the left side at "c1", respectively. $e_{\uparrow}^{g}$ and $e_{\downarrow}^{g}$ are the edge strengths of the vertical direction for the top side and the bottom side, respectively. If the value of $|e_{\rightarrow}^{g} - e_{\leftarrow}^{g}|$ is larger than D_{eg}, it means the edge strengths of the right and the left are significantly different, otherwise, the two values have no large difference. For the vertical side, the same principle can be applied to decide whether the edge strengths of the top side and the bottom side are different enough by comparing $|e_{\uparrow}^{g} - e_{\downarrow}^{g}|$ with D_{eg}.

In Eq. (6), there are five situations and each situation has its own method to select the neighboring pixels for interpolating the missing green value. The first situation corresponds to a horizontally half-side uniform configuration which satisfies the following four conditions: (1) the horizontal edge strength should be relatively smaller than the vertical edge strength (i.e. $e_{|}^{g}/e_{-}^{g} > R$), (2) the total horizontal and vertical edge strength should be not too small (i.e. $e_{|}^{g} + e_{-}^{g} > T_1$), (3) the horizontal edge strength should be small enough (i.e. $e_{-}^{g} < T_2$), and (4) only half of the horizontal direction (either the right-half or the left-half) is uniform and the other half is non-uniform (i.e. $|e_{\rightarrow}^{g} - e_{\leftarrow}^{g}| > D_{eg}$). If all above four conditions are satisfied, then we estimate the missing value $\hat{d}^{g}$ by the value of d_{w-}^{a}.

The second, third, and fourth situations correspond to a vertically half-side uniform configuration, a horizontally two-side uniform configuration, and a vertically two-side uniform configuration, respectively. If the green missing pixel does not belong to the above four situations, it belongs to the fifth situation which corresponds to either a non-uniform or a uniform configuration in both horizontal and vertical directions. Readers can easily understand the required conditions of each situation because they are similar to the condition illustration of the first situation. In the fifth situation the individual green color continuity is based on the respective vertical and horizontal direction to give each direction the suitable weight. So that the central green missing value can be interpolated according to d_{-}^{a}, $d_{|}^{a}$ and their weights $w_{|}^{g}$ and w_{-}^{g} by the following Equation.

$$w_{|}^{g} = \frac{e_{-}^{g}}{e_{|}^{g} + e_{-}^{g}}, \quad w_{-}^{g} = 1 - w_{|}^{g}. \tag{7}$$

3. Demosaicking Procedure of the *R-G*/*B-G* Color Difference Planes

Let *R-G* denote the color difference plane of the red plane and the demosaicked green plane and *B-G* denote the color difference plane of the blue plane and the demosaicked green plane. That is $R\text{-}G = R\text{-}\bar{G}$ and $B\text{-}G = B\text{-}\bar{G}$. Both *R-G* and *B-G* inherently are low-pass signal which can be utilized to reduce the estimated errors of the demosaicked images, and the ECDB algorithm uses them to reconstruct the red and blue planes, individually. Since both *R-G* and *B-G* are derived by similar operations, only the derivation of *R-G* is described here. Because there are many red-missing pixels in the red plane *R*, many pixels will accordingly have no values in the *R-G* plane. These pixels are called the "missing *R-G* pixels" which can be categorized into three classes: diagonal class, vertical class, and horizontal class. A pixel is attributed to (1) the horizontal class if its left and right *R-G* pixels have values; (2) the vertical class if its top and bottom *R-G* pixels have values; and (3) the diagonal class if otherwise. Because in the design when reconstructing a *R-G* pixel value of an either horizontal-class or vertical-class pixel, the values of some pixels belonging to diagonal class are referenced; but the *R-G* pixel value of a diagonal-class pixel can be estimated directly without referencing the values of horizontal-class and vertical-class pixels. Therefore, the diagonal-class pixels should be estimated first, and the pixels of the other two classes later.

4. Value Estimation of the Missing Diagonal-Class *R-G* Pixels

In order to describe the estimated value of a missing *R-G* pixel, Fig. 3 is provided to show the geometric relations of the missing *R-G* pixels. For estimating the *R-G* value of B_1, let $e_{|}^{a}$, e_{-}^{a}, $e_{/}^{a}$ and $e_{\backslash}^{a}$ be the edge strengths in the vertical, horizontal, diagonal and reverse diagonal directions, respectively. The four edge strengths (e_{i}^{a}, $\forall i \in \{ |, -, /, \backslash \}$) are defined as

$$\begin{aligned}
&e_{|}^{a} = e_{|}^{rg} + e_{|}^{rb}, \quad e_{/}^{a} = \frac{e_{\rightarrow\uparrow}^{r} + e_{\leftarrow\downarrow}^{r}}{2} + e_{/}^{rb}, \\
&e_{-}^{a} = e_{-}^{rg} + e_{-}^{rb}, \quad e_{\backslash}^{a} = \frac{e_{\leftarrow\uparrow}^{r} + e_{\rightarrow\downarrow}^{r}}{2} + e_{\backslash}^{rb}. \\
&e_{|}^{rb} = |2*B_1 - B_6 - B_2|, \quad e_{-}^{rb} = |2*B_1 - B_4 - B_8|, \\
&e_{/}^{rb} = |2*B_1 - B_7 - B_3|, \quad e_{\backslash}^{rb} = |2*B_1 - B_5 - B_9|, \\
&e_{|}^{rg} = |G_{13} - G_1| + |G_1 - G_3| + |G_3 - G_{19}|, \\
&e_{-}^{rg} = |G_{22} - G_4| + |G_4 - G_2| + |G_2 - G_{16}|.
\end{aligned} \tag{8}$$

Let $e_{\rightarrow\uparrow}^{r}$, $e_{\leftarrow\downarrow}^{r}$, $e_{\leftarrow\uparrow}^{r}$ and $e_{\rightarrow\downarrow}^{r}$ be the edge strengths of the missing *R-G* pixels on the top-right, the bottom-left, the

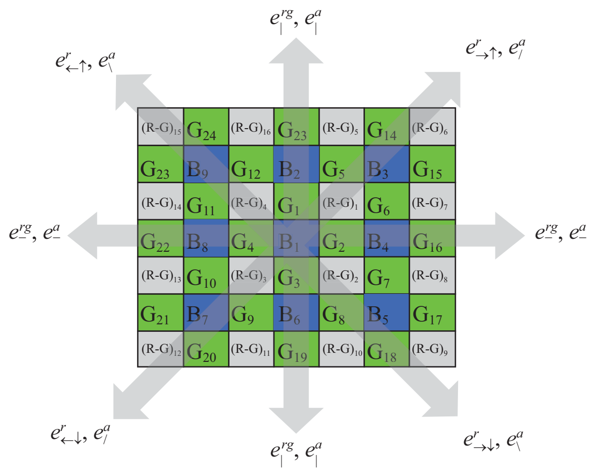

Fig. 3. The to-be-estimated *R-G* value on the blue sample B_1.

top-left, and the bottom-right direction, respectively. The values of $e^r_{\rightarrow\uparrow}$, $e^r_{\leftarrow\downarrow}$, $e^r_{\leftarrow\uparrow}$ and $e^r_{\rightarrow\downarrow}$ can be given by

$$e^r_{\rightarrow\uparrow} = |R_3 - R_1| + 2*|R_1 - R_6|,\ e^r_{\leftarrow\uparrow} = |R_4 - R_2| + 2*|R_4 - R_{15}|,$$
$$e^r_{\leftarrow\downarrow} = |R_3 - R_1| + 2*|R_3 - R_{12}|,\ e^r_{\rightarrow\downarrow} = |R_4 - R_2| + 2*|R_2 - R_9|. \quad (9)$$

Let $(R\text{-}G)_1$, $(R\text{-}G)_2$, $(R\text{-}G)_3$ and $(R\text{-}G)_4$ be the values of the diagonal and reverse diagonal *R-G* pixels around B_1, $d^{r-g}_{/}$ be the average of $(R\text{-}G)_1$ and $(R\text{-}G)_3$, $d^{r-g}_{\backslash}$ be the average of $(R\text{-}G)_2$ and $(R\text{-}G)_4$. $w^r_{\rightarrow\uparrow}$, $w^r_{\leftarrow\downarrow}$, $w^r_{\leftarrow\uparrow}$ and $w^r_{\rightarrow\downarrow}$ be the weight of $(R\text{-}G)_1$, $(R\text{-}G)_2$, $(R\text{-}G)_3$ and $(R\text{-}G)_4$, respectively. These 6 parameters ($d^{r-g}_{/}$, $d^{r-g}_{\backslash}$, $w^r_{\rightarrow\uparrow}$, $w^r_{\leftarrow\downarrow}$, $w^r_{\leftarrow\uparrow}$ and $w^r_{\rightarrow\downarrow}$) are calculated by

$$d^{r-g}_{/} = \frac{(R-G)_1 + (R-G)_3}{2},\ d^{r-g}_{\backslash} = \frac{(R-G)_2 + (R-G)_4}{2}.$$
$$w^r_{\rightarrow\uparrow} = \frac{e^r_{\leftarrow\downarrow}}{e^r_{\rightarrow\uparrow} + e^r_{\leftarrow\downarrow}},\ w^r_{\leftarrow\downarrow} = 1 - w^r_{\leftarrow\downarrow},$$
$$w^r_{\leftarrow\uparrow} = \frac{e^r_{\rightarrow\downarrow}}{e^r_{\leftarrow\uparrow} + e^r_{\rightarrow\downarrow}},\ w^r_{\rightarrow\downarrow} = 1 - w^r_{\leftarrow\uparrow}. \quad (10)$$

If the estimated value on the diagonal direction has high attribute consistence for both sides (top-right and bottom-left), n equal weight value is given to both sides (i.e. $d^{r-g}_{/}$); otherwise, different weight values are given to both sides (i.e. $w^r_{\rightarrow\uparrow} \times (R\text{-}G)_1 + w^r_{\leftarrow\downarrow} \times (R\text{-}G)_3$). If the estimated value on the reverse diagonal direction has high attribute consistence for both sides (top-left and bottom-right), an equal weight value is given to both sides (i.e. $d^{r-g}_{\backslash}$); otherwise, different weight values are given to both sides (i.e. $w^r_{\leftarrow\uparrow} \times (R\text{-}G)_4 + w^r_{\rightarrow\downarrow} \times (R\text{-}G)_2$). When there is no significant consistency direction either on diagonal or reverse diagonal direction, the individual *R-G* plane continuity is based on the respective top-right, bottom-left, top-left and bottom-right directions to give each direction the suitable weight values. So that we interpolate the missing *R-G* value according to $(R\text{-}G)_1$, $(R\text{-}G)_2$, $(R\text{-}G)_3$ and $(R\text{-}G)_4$ and their weights $w^a_{\rightarrow\uparrow}$, $w^a_{\rightarrow\downarrow}$, $w^a_{\leftarrow\downarrow}$ and $w^a_{\leftarrow\uparrow}$ can given by

$$w^a_{\rightarrow\uparrow} = \frac{1}{1 + |B_1 - B_3| + |G_1 - G_5| + |G_2 - G_6|},$$
$$w^a_{\rightarrow\downarrow} = \frac{1}{1 + |B_1 - B_5| + |G_2 - G_7| + |G_3 - G_8|},$$
$$w^a_{\leftarrow\downarrow} = \frac{1}{1 + |B_1 - B_7| + |G_3 - G_9| + |G_4 - G_{10}|},$$
$$w^a_{\leftarrow\uparrow} = \frac{1}{1 + |B_1 - B_9| + |G_4 - G_{11}| + |G_1 - G_{12}|} \quad (11)$$

The estimated $\hat{d}^{r-g}_{/}$ value of a diagonal-class missing pixel (B_1) becomes

$$\hat{d}^{r-g}_{/} = \begin{cases} w^r_{\rightarrow\uparrow} \times (R-G)_1 + w^r_{\leftarrow\downarrow} \times (R-G)_3, & \text{if } \left|e^r_{\rightarrow\uparrow} - e^r_{\leftarrow\downarrow}\right| \ge T_d \text{ and } \left|e^r_{\rightarrow\uparrow} + e^r_{\leftarrow\downarrow}\right| < T_2 \text{ and } \\ & \max_{\forall i \in \{|,-,/,\backslash\}} e^a_i / e^a_{/} > T_d \text{ and } e^a_{/} = \min_{\forall i \in \{|,-,/,\backslash\}} e^a_i; \\ w^r_{\leftarrow\uparrow} \times (R-G)_4 + w^r_{\rightarrow\downarrow} \times (R-G)_2, & \text{if } \left|e^r_{\leftarrow\uparrow} - e^r_{\leftarrow\downarrow}\right| \ge T_d \text{ and } \left|e^r_{\leftarrow\uparrow} + e^r_{\rightarrow\downarrow}\right| < T_2 \text{ and } \\ & \max_{\forall i \in \{|,-,/,\backslash\}} e^a_i / e^a_{\backslash} > T_d \text{ and } e^a_{\backslash} = \min_{\forall i \in \{|,-,/,\backslash\}} e^a_i; \\ d^{r-g}_{/}, & \text{if } \max_{\forall i \in \{|,-,/,\backslash\}} e^a_i / e^a_{/} > T_d \text{ and } e^a_{/} = \min_{\forall i \in \{|,-,/,\backslash\}} e^a_i; \\ d^{r-g}_{\backslash}, & \text{if } \max_{\forall i \in \{|,-,/,\backslash\}} e^a_i / e^a_{\backslash} > T_d \text{ and } e^a_{\backslash} = \min_{\forall i \in \{|,-,/,\backslash\}} e^a_i; \\ d^{r-g}_{s}, & \text{otherwise.} \end{cases} \quad (12)$$

In Eq. (12), T_d and T_2 are two threshold values. If the edge strength $|e^r_{\rightarrow\uparrow} - e^r_{\leftarrow\downarrow}|$ >= T_d, it means the edge strengths of the top-right and the bottom-left directions have a significant difference. If the edge strength $|e^r_{\rightarrow\uparrow} + e^r_{\leftarrow\downarrow}|$ < T_2, it means the missing *R-G* pixel is located at a non-complex area. $\max_{\forall i \in \{|,-,/,\backslash\}} e^a_i$ and $\min_{\forall i \in \{|,-,/,\backslash\}} e^a_i$ denote the maximum and the minimum of $e^a_{|}$, e^a_{-} , $e^a_{/}$ and $e^a_{\backslash}$, respectively. $\max_{\forall i \in \{|,-,/,\backslash\}} e^a_i / e^a_{/} > T_d$ and $e^a_{/} = \min_{\forall i \in \{|,-,/,\backslash\}} e^a_i$ means the region around B_1 has a high continuity along the diagonal direction and it is a non-complex area, Similarly, $\max_{\forall i \in \{|,-,/,\backslash\}} e^a_i / e^a_{\backslash} > T_d$ and $e^a_{\backslash} = \min_{\forall i \in \{|,-,/,\backslash\}} e^a_i$ means the region around B_1 has a high continuity along the reverse diagonal direction and it is a non-complex area.

In Eq. (12), there are five situations and each situation has its own method to select the neighboring pixels for interpolating the missing *R-G* value. The first situation corresponds to a diagonally half-side uniform configuration which satisfies the following four conditions: (1) only half of the diagonal direction (either the top-right-half or the bottom-left-half) is uniform and the other half is non-uniform (i.e. $|e^r_{\to\uparrow} - e^r_{\leftarrow\downarrow}| >= T_d$), (2) the diagonal edge strength should be small enough (i.e. $|e^r_{\to\uparrow} + e^r_{\leftarrow\downarrow}| < T_2$), (3) the diagonal edge strength should be relatively smaller than the maximum strengths (i.e. $\max_{\forall i \in \{|,-,/,\backslash\}} e^a_i / e^a_/ > T_d$), (4) the diagonal edge strength should be the smallest of the four direction edge strengths (i.e. $e^a_/ = \min_{\forall i \in \{|,-,/,\backslash\}} e^a_i$). If all above four conditions are satisfied, then the missing *R-G* value is estimated by $w^r_{\to\uparrow} \times (R-G)_1 + w^r_{\leftarrow\downarrow} \times (R-G)_3$. The second, third, and fourth situations correspond to a reverse diagonally half-side uniform configuration, a diagonally two-side uniform configuration, and a reverse diagonally two-side uniform configuration, respectively. If the missing *R-G* pixel does not belong to any of the above four situations, it belongs to the fifth situation which corresponds to either a non-uniform or a uniform configuration in both diagonal and reverse diagonal directions. Similar to the explanation of the first situation, the required conditions of other situations are clear. In the fifth situation the individual *R-G* pixel continuity is based on the respective diagonal and reverse diagonal directions to give each direction the suitable weight. So that the missing *R-G* value can be interpolated according to $(R\text{-}G)_1$, $(R\text{-}G)_2$, $(R\text{-}G)_3$ and $(R\text{-}G)_4$ and their corresponding weights $w^a_{\to\uparrow}$, $w^a_{\to\downarrow}$, $w^a_{\leftarrow\downarrow}$ and $w^a_{\leftarrow\uparrow}$ by the following:

$$d_s^{r-g} = \frac{(R-G)_1 \times w^a_{\to\uparrow} + (R-G)_2 \times w^a_{\to\downarrow} + (R-G)_3 \times w^a_{\leftarrow\downarrow} + (R-G)_4 \times w^a_{\leftarrow\uparrow}}{\sum_{\forall j \in \{(\to\uparrow),(\leftarrow\downarrow),(\leftarrow\uparrow),(\to\downarrow)\}} w^a_j}. \tag{13}$$

where the d_s^{r-g} is the ratio of the weighted summation of $(R\text{-}G)_1$, $(R\text{-}G)_2$, $(R\text{-}G)_3$ and $(R\text{-}G)_4$ and the summation of $w^a_{\to\uparrow}$, $w^a_{\to\downarrow}$, $w^a_{\leftarrow\downarrow}$ and $w^a_{\leftarrow\uparrow}$.

5. Value Estimation of the Missing Vertical-class *R-G* pixels

Let $w_|^{r-g}$ and w_-^{r-g} be the weights associated with the vertical and horizontal directions, respectively, and they are defined as

$$e_-^{r-g} = |2*(R-G)_4 - (R-G)_8 - (R-G)_2| + |2*(R-G)_2 - (R-G)_4 - (R-G)_6|,$$

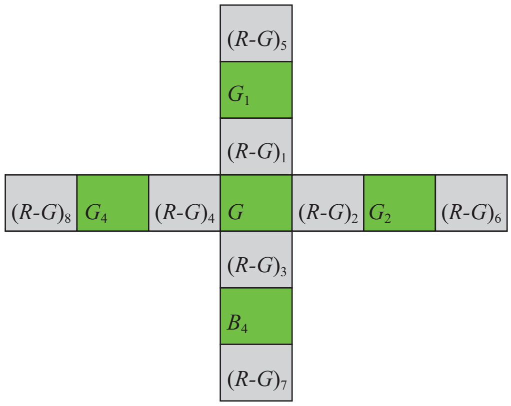

Fig. 4. Related pixels for estimating the *R-G* value of a missing vertical-class pixel at location *G*.

$$e_|^{r-g} = |2*(R-G)_1 - (R-G)_5 - (R-G)_3| + |2*(R-G)_3 - (R-G)_1 - (R-G)_7|.$$

$$w_|^{r-g} = 0.8 \times \frac{e_-}{e_| + e_-}, \quad w_-^{r-g} = 1 - w_|^{r-g}. \tag{14}$$

where e_-^{r-g} and $e_|^{r-g}$ denote the individual edge strengths of the horizontal and vertical directions. The larger e_-^{r-g} is compared to $e_|^{r-g}$, the larger $w_|^{r-g}$ will be. In figure 4, the *R-G* values of $(R\text{-}G)_1$, $(R\text{-}G)_3$, $(R\text{-}G)_5$ and $(R\text{-}G)_7$ are the genuine *R-G* values, but the *R-G* values of $(R\text{-}G)_2$, $(R\text{-}G)_4$, $(R\text{-}G)_6$ and $(R\text{-}G)_8$ are the estimated ones by using the method introduced in Section 2.4. Because the estimated *R-G* values are less reliable than the genuine *R-G* values, they have a smaller contribution in computing $\hat{d}_|^{r-g}$. Therefore, $w_|^{r-g}$ is multiplied by 0.8 in Eq. (14). The missing *R-G* value at the *G* sample location (Fig. 4) is estimated by

$$\hat{d}_|^{r-g} = \begin{cases} \dfrac{(R-G)_4 + (R-G)_2}{2}, & \text{if } \dfrac{e_|^{r-g}}{e_-^{r-g}} > R, \\ \dfrac{(R-G)_1 + (R-G)_3}{2}, & \text{if } \dfrac{e_-^{r-g}}{e_|^{r-g}} > R, \\ w_|^{r-g} * \dfrac{(R-G)_1 + (R-G)_3}{2} + w_-^{r-g} * \dfrac{(R-G)_4 + (R-G)_2}{2}, & \text{otherwise.} \end{cases} \tag{15}$$

where $e_|^{r-g}$ and e_-^{r-g} are the edge strengths in the vertical and horizontal directions. If $e_|^{r-g} / e_-^{r-g} > R$, it means there is horizontal texture on the location *G*; if $e_-^{r-g} / e_|^{r-g} > R$, it means there is vertical texture on the location *G*. Since the derivation

Fig. 5. Test images (from left to right, top to down, are image No.1 to No.24, respectively).

of the missing vertical-class and the horizontal-class pixels are similar, the interpolation method is used to estimate the missing vertical-class pixels.

After the interpolation operations mentioned above have been processed, the full *R-G* and *B-G* planes can be constructed. Accordingly, the demosaicked red plane $(\bar{R})$ can be produced from the *R-G* plane because $\bar{R} = R\text{-}G + \bar{G}$. Similarly, the demosaicked blue plane $(\bar{B})$ can also be produced in the same way. Therefore, a full-color demosaicked image can eventually be constructed from the $\bar{R}$, $\bar{G}$ and $\bar{B}$ planes.

III. EXPERIMENTS

In these experiments; 24 test images were compared, as shown in Fig. 5, which are contained in the Kodak 3CCD image database [1]. Each test image is a 24-bit full-color image containing one 8-bit value for each color and consisting of 512×768 pixels.

The test images were produced by preserving only one color component and abandoning the other two color components for each pixel from the original full color images. All the test images are represented as the Bayer CFA pattern. In our experiments, all test images were interpolated into demosaicked full-color images and their simulation results were compared by both the mean square error (MSE) and the peak signal-to-noise ratio (PSNR). MSE and PSNR are formulated as

$$MSE = \frac{|I_0 - I_d|^2}{3 \times H \times W}, \quad PSNR = 10 \times \log_{10}\left(\frac{255^2}{(MSE)}\right). \quad (16)$$

Table 2. Performance comparison of different methods.

Image No	BI		ACPI		ECI		Proposed ECDB	
	PSNR	MSE	PSNR	MSE	PSNR	MSE	PSNR	MSE
1	23.230	154.910	33.780	27.232	33.816	27.007	*35.844*	*17.159*
2	33.090	31.921	38.850	8.474	39.120	7.963	*40.286*	*6.916*
3	34.360	23.828	40.660	5.586	40.211	6.194	*41.738*	*4.493*
4	33.660	27.995	39.160	7.890	39.147	7.913	*40.754*	*6.631*
5	26.720	138.382	35.040	20.374	35.044	20.355	*36.708*	*14.073*
6	27.730	109.668	35.110	20.048	34.656	22.259	*36.978*	*13.267*
7	33.470	29.247	40.850	5.347	40.448	5.866	*41.863*	*4.415*
8	23.640	281.242	32.340	37.939	30.274	61.053	*33.975*	*26.588*
9	32.510	36.482	40.330	6.027	39.427	7.420	*41.581*	*4.617*
10	32.320	38.114	40.020	6.473	39.855	6.723	*41.319*	*4.962*
11	29.300	76.398	36.340	15.104	36.336	15.118	*38.272*	*9.794*
12	32.900	33.349	40.720	5.509	39.687	6.988	*41.825*	*4.402*
13	23.950	261.867	29.930	66.082	31.034	51.248	*32.097*	*40.271*
14	29.280	76.750	35.810	17.064	35.102	20.087	*38.836*	*14.013*
15	31.500	46.034	37.440	11.724	38.200	9.842	*38.734*	*9.152*
16	31.370	47.433	38.690	8.792	38.243	9.746	*40.921*	*5.342*
17	31.960	41.408	38.670	8.832	39.177	7.859	*40.183*	*6.272*
18	27.920	104.974	33.740	27.484	34.934	20.877	*35.320*	*19.437*
19	28.160	99.330	37.310	12.080	35.046	20.346	*39.062*	*8.228*
20	30.360	59.852	38.220	9.797	38.204	9.833	*39.842*	*7.046*
21	28.590	89.966	35.350	18.971	35.587	17.965	*37.285*	*12.356*
22	30.540	57.422	36.520	14.490	36.214	15.550	*37.533*	*11.968*
23	35.300	19.190	42.050	4.056	41.478	4.627	*42.641*	*3.676*
24	26.640	140.955	32.020	40.839	32.674	35.133	*33.302*	*31.426*
Avg.	30.062	64.103	36.828	13.901	36.830	13.493	*38.537*	*11.938*

where I_o and I_d are the original full-color image and its demosaicked full-color image, respectively; H and W are the height and the width of the original full-color image, respectively. For a demosaicked image, high fidelity implies high PSNR and small MSE measurements. Table 2 lists the measurement results of MSE and PSNR regarding to ECDB, BI, ACPI, and ECI [8] by using all of the 24 test images.

Figs 6, 7 and 8 demonstrate the demosaicked results obtained by different demosaicking methods. In the three figures, both color artifact and zipper effect are mainly displayed in the fine-edge regions. Obviously, the ECDB algorithm provides the lowest color artifacts and the zipper effect for the edge region in the demosaicked result as shown in Fig. 6(e), Fig. 7(e) and Fig. 8(e). In the simulation results, the ECDB algorithm performed better and chose suitable samples to interpolate missing pixels to reduce false colors, zipper effects, and then demosaicked images were visually more pleasing.

IV. CONCLUSION

In this paper, an effective CFA demosaicking interpolation algorithm is proposed which is called "Effective Color-Difference-Based Interpolation" (ECDB). The ECDB algorithm has provided pleasing results, and its performance is

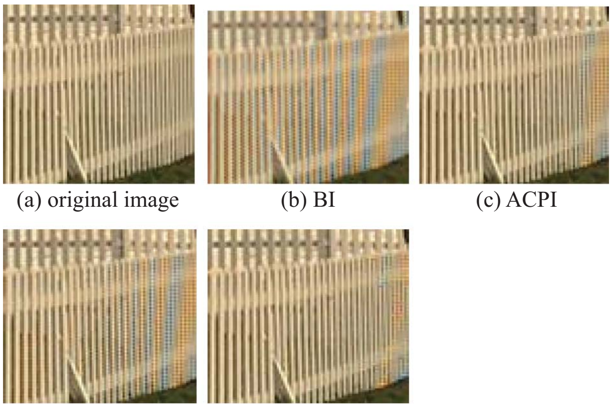

(a) original image (b) BI (c) ACPI
(d) ECI (e) proposed ECDB

Fig. 6. Enlarged parts of the demosaicked image corresponding to the fence picture: (a) the original image, (b) BI, (c) ACPI, (d) ECI, and (e) the proposed ECDB.

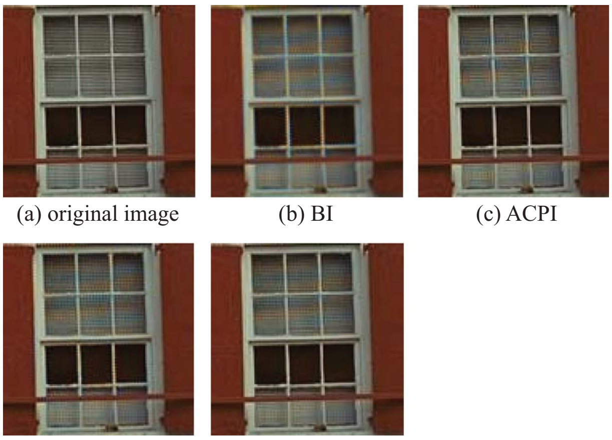

(a) original image (b) BI (c) ACPI
(d) ECI (e) proposed ECDB

Fig. 7. Enlarged parts of the demosaicked image corresponding to the brickwood: (a) the original image, (b) GBI, (c) ACPI, (d) ECI, and (e) the proposed ECDB.

much better than the previous works shown in the experiments. Because the demosaicked image produced by the ECDB algorithm still has a few false colors at the high-contrast edge pixels, obtaining more a correct color at the high-contrast edge pixels has become the main research direction for future work.

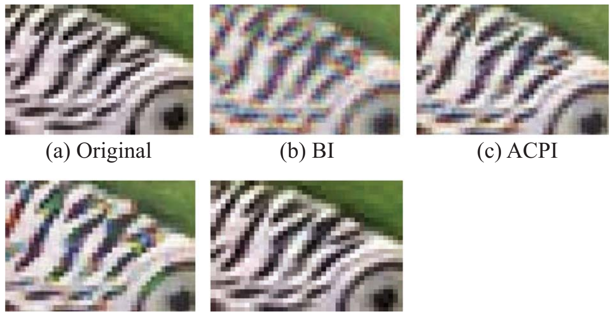

(a) Original (b) BI (c) ACPI
(d) ECI (e) proposed ECDB

Fig. 8. Enlarged parts of the demosaicked image corresponding to the Parrots: (a)The original image, (b) BI, (c) ACPI, (d) ECI, and (e) the proposed ECDB.

ACKNOWLEDGMENTS

The author acknowledges the financial support of the National Science Council (NSC 100-2221-E-216-031 and NSC 100-2622-E-216-001-CC3), ROC.

REFERENCES

1. Kodak Lossless True Color Image Suite, http://r0k.us/graphics/kodak/.
2. Lee, B., "Performance comparison of various interpolation methods for color filter arrays," *Proceedings of the IEEE International Symposiumon Industrial Electronics*, Vol. 1, pp. 232-236 (2001).
3. Longere, P., Zhang, X., Delahunt, P. B., and Brainard, D. H., "Perceptual assessment of demosaicing algorithm performance," *Proceedings of the IEEE*, Vol. 90, No. 1, pp. 123-132 (2002).
4. Lukac, R., Martin, K., and Plataniotis, K. N., "Demosaicked image post-processing using local color ratios," *IEEE Transactions on Circuits and Systems for Video Technology*, Vol. 14, No. 6, pp. 914-920 (2004).
5. Lukac, R. and Plataniotis, K. N., "Data-adaptive filters for demosaicking: a framework," *IEEE Transactions on Consumer Electronics*, Vol. 51, No. 2, pp. 560-570 (2005).
6. Lukac, R. and Plataniotis, K. N., "Color filter arrays: Design and performance analysis," *IEEE Transactions on Consumer Electronics*, Vol. 51, No. 4, pp. 1260-1267 (2005).
7. Lukac, R., Plataniotis, K. N., Hatzinakos, D., and Aleksic, M., "A novel cost effective demosaicing approach," *IEEE Transactions on Consumer Electronics*, Vol. 50, No. 1, pp. 256-261 (2004).
8. Lukac, R., Plataniotis, K. N., Hatzinakos, D., and Aleksic, M., "A new CFA interpolation framework," *Signal Processing*, Vol. 86, No. 7, pp. 1559-1579 (2006).
9. McKinley, S. and Levine, M., "Cubic spline interpolation," Math 45: Linear Algebra (1998).
10. Pei, S. C. and Tam, I. K., "Effective color interpolation in CCD color filter arrays using signal correlation," *IEEE Transactions on Circuits and Systems for Video Technology*, Vol. 13, No. 6, pp. 503-513 (2003).
11. Tsai, C. Y. and Song, K. T., "A new edge-adaptive demosaicking algorithm for color filter arrays," *Image and Vision Computing*, Vol. 25, No. 9, pp. 1495-1508 (2007).